

Core And Log NMR Measurements Indicate Reservoir Rock Is Altered By OBM Filtrate.

John Shafer¹, Jiansheng Chen², Mark Flaum², George Hirasaki², Austin Boyd³, Christian Straley³, Tim Borbas⁴, Chuck Devier⁵

¹Reservoir Management Group, Houston, TX, USA

²Rice University, Houston, TX, USA

³Schlumberger-Doll Research, Ridgefield, Cn, USA

⁴ConocoPhillips, Houston, TX, USA

⁵PTS Labs, Houston, TX, USA

ABSTRACT

A core-to-log NMR calibration program for a Gulf of Mexico deep-water reservoir indicates the near wellbore rock wettability is intermediate-wet to oil-wet with enhanced relaxation that results in significant internal gradients (150 to 200 Gauss/cm). This affects the validity of certain aspects of NMR well log interpretation because the response is usually based on the assumption that the formation is water-wet and the magnetic field gradient is equal to that designed for the logging tool.

NMR logs were obtained on nine wells including the cored well and logging-while- drilling (LWD) NMR on an offset well followed by about a week later by wireline NMR log. LWD NMR wiper pass logs run 2.5 days after drilling indicate a longer relaxing T_2 peak than the wireline log run 7 days after drilling. These observations are consistent with the OBMF filtrate invasion of the formation causing enhanced relaxation of the OBMF by wettability alteration and paramagnetic particle invasion.

Fresh state and OBMF at S_{wi} (connate water) core plug saturation states have NMR T_2 distributions at reservoir confining stress and temperature similar to the wireline log NMR over the same depth intervals. Cores at S_{wi} saturated with OBMF have oil relaxation rates much faster than the bulk OBMF relaxation rate and the OBMF T_2 mode in the cores does not vary significantly with temperature. Both of these observations indicate that the main mechanisms for oil relaxation are surface relaxation and internal gradients and indicating oil is wetting some portion of the rock surface. The T_1 and T_2 distributions of the OBMF depend on whether the whole mud is pressed or a supernatant is filtered. The filtered OBMF was found to contain 0.08 micron paramagnetic particles.

Diffusion editing and CPMG T_2 distributions with multiple echo spacings indicate high internal gradients, in the range of 50 to 100 G/cm for extracted plugs and over 150 G/cm for fresh-state plugs. Thin sections and SEM photomicrographs and XRD show that the rocks often

contain “trains” of heavy minerals (iron minerals) and shale laminations with little evidence of dispersed clays. The drilling mud solids had a high magnetic susceptibility and the magnetic fraction was identified to contain both iron and magnetite.

There is ample evidence the fast relaxation of OBMF is a result of diffusion relaxation with large internal gradients and surface relaxation caused by OBMF alteration. Laboratory investigation is ongoing to determine whether the alteration is caused by the OBM surfactant additives or submicron paramagnetic particulate material in the OBMF.

INTRODUCTION

ConocoPhillips over the past several years has drilled 9 wells and 4 sidetracks using synthetic oil base muds (OBM) in a deepwater field in the Gulf of Mexico. Seven of these wells have included CMR nuclear magnetic resonance (NMR) logs and reservoir sands in one of the wells were cored. PVT data on downhole fluid samples indicated that the reservoir oil and the synthetic base oil used in the OBM should have an NMR spin-spin (T_2) relaxation time of about 1000 ms at reservoir conditions, yet the NMR logs indicate a peak at about 150 ms. The observed shift in the NMR logs for hydrocarbon (HC) T_2 peak to the left of the bulk HC peak could be the result of rock wettability or rock magnetic field gradients or a combination of both. To help understand the cause of this apparent discrepancy initially two laboratory programs were started, one by SDR to look at the NMR response of the live and dead HC fluids and the other at PTS Labs to for a core-to-log NMR study. As we proceeded with these studies we encountered unusual results that were of interest to Rice University Consortium on Porous Media and they became involved. The results reported in this paper are from a cooperative research program between Rice University, Schlumberger Doll Research, PTS Labs International, ConocoPhillips, and Reservoir Management Group.

The surfactants in synthetic oil base muds (OBM) are known to alter rock wettability to a more oil-wet state (Marschall and Coats, 1997; Chen, et al., 2004). The surfactants (emulsifiers and oil wetting agents) are added to stabilize the water-in-oil emulsion and to ensure that the drilled cuttings and density control particles are oil-wet. Potentially these surfactant additives to the synthetic base oil can invade the formation and alter the formation rock wettability to a more oil wet state. McCaffery et. al states that this is a well-known problem. (McCaffery, 2002). If the wettability of the rock in the near well bore region of the formation is altered to a more oil-wet state then a portion of the non-mobile (connate) water potentially will be mobilized resulting in artificially low water saturations. If the depth of invasion of the OBM filtrate is limited, then deep reading resistivity measurements should not be altered, however the core water saturation as determined by Dean-Stark extraction potentially will be lower than the non-invaded rock.

Rock internal magnetic field gradients result in a strong echo-spacing-dependent shortening of the NMR T_2 relaxation time distribution and large T_1/T_2 ratios. The internal field gradient are the result of magnetic susceptibility contrast with the surrounding pore fluids. Strong internal gradients are often observed in authogenic (diagenetic) clays such as pore-lining chlorite. (Zhang, et al., 2000, 2001, and 2003, Rueslatten, et al., 1998)

Geologic Description The reservoir of interest consists of Gulf of Mexico Pleistocene age stacked turbidite sand/shale sediment, deposited as a series of laterally and vertically amalgamated channels. The reservoir unit displays an overall fining upward trend, with increased structural shale present in the upper sand facies and more massive sand placement with ripple fabric in the lower sand facies. A log section of the reservoir showing the conventionally cored interval is shown in Figure 1. The CMR log is in the right most track and indicates that the longest relaxing peak that is assume to be some mixture of reservoir live oil and OBMF is typically between 100 to 200ms for the sand interval. The regional oil water contact (OWC) is interpreted to be 800 feet below the base of the cored interval. Thus the cored interval is assumed to be at or near irreducible saturation.

About 250 feet of core were recovered and one plug per foot was taken for routine core analysis, consisting of Dean-Stark water saturations, permeability, porosity, and laser particle size analysis. The permeability and porosity data are in the 4th and 5th tracks of the log in Figure 1. The special core analysis program had a total of 13 air-brine capillary pressure measurements. A comparison of air perm versus brine saturation obtained from the Dean-Stark extraction and that predicted from the capillary pressure

measurements indicate the Dean-Stark saturation are often less than predicted by capillary pressure.

Deposited in a deep-water environment, the pore geometry is largely controlled by particle size, as moderate temperatures (160°F) and recent geologic deposition have inhibited development of authogenic cements. Particle size data from the cored reservoir unit indicate that higher quality flow units are comprised of very fine-grained sediment, with the poorer flow units dominated by medium silts. As illustrated in Figure 2, much of the reservoir is heterogeneous on the core scale, slabbed core picture on the left, and heterogeneous on the plug scale, thin section, low magnification photo in the middle. Shale laminations on the mm scale are obvious from the thin section photo. The higher magnification photomicrograph on the right shows the presence of opaque heavy mineral "trains". Petrographic point analysis of the heavy minerals was about 4 to 5% as non-opaque and 2-3% as opaque and include magnetite, magnetite-ilmenite, epidote, tourmaline, zircon, and garnet. Whole rock XRD typically reported the following: Quartz =55%, Plagicoclase = 13%, K-feldspar = 10%, calcite = 5%, dolomite = 5%, pyrite = 1%, and a total clay of 11%. XRD analysis on the clay size fraction indicate that this 11% total clay is typically composed of 1% Kaolinite, 1% chlorite, 2% illite, 7% mixed layer clay. XRD analysis on a heavy liquid sink fraction confirms the presence of magnetite. The clays are concentrated in the shale laminations with very little dispersed matrix or structural clays identified. Thus the formation contains localized iron minerals but little to no dispersed clays.

PROTOCOL

Rock and fluid sample NMR measurements were performed at two labs, PTS Labs and the Chemical Engineering Department at Rice University. The initial core-to-log NMR calibration program consisted of six core plugs. The samples were received in one of two conditions: four samples had been miscibly extracted, the other two of samples had not been previously analyzed and were received frozen in a "fresh or native state".

PTS Labs All NMR measurements were performed using a MARAN Ultra Magnetic Resonance Core Analyzer spectrometer operating at approximately 2 MHz. The core plugs were packaged in an NMR compatible material to minimize grain and fluid loss during testing. The plugs were tested in a commercially available NMR compatible core holder with a working pressure of 5000 psi. at 250 degrees F. Confining stress and temperature was applied using a recirculating pressure system filled with a proton free fluorine based overburden fluid. Blank measurements were made periodically throughout the testing sequence to insure that no contaminates, which generate an NMR response, had been introduced to the test apparatus.

The T_2 measurements were obtained using a CPMG pulse sequence. Multiple inter-echo spacing of 0.30, 0.60, and 1.20 ms were selected for each sample. A sufficient number of echo trains were used to generate a signal to noise ratio of 200:1. Delay times between each pulse sequence were adjusted to allow complete recovery of the sample. Hydrogen index calibrations of all test brines and oils were performed on known volumes at the appropriate test stress and temperature. Relaxation time distributions were computed by multi-exponential inversion of the echo data with 51 preset decay times logarithmically spaced between 0.1 ms and 10,000 ms. Multiple inter-echo spacing NMR T_2 measurements on a water sample indicate no significant inhomogeneity in the NMR spectrometer's B_0 field.

Rice University NMR T_1 , T_2 and diffusion editing measurements were made at room temperature with a Maran-2 spectrometer (Resonance, Inc.). T_1 and T_2 were measured by IR and CPMG pulse sequences, respectively. The signal to noise ratio for T_1 , T_2 measurements is about 100. A non-linear least square inversion method (Chuah, 1996, Huang, 1997) was used to estimate the multi-exponential relaxation time distributions. Diffusion Editing (DE) measurements were carried out at 9 diffusion times. 3000 echoes with echo spacing of 400 μ s were collected at each diffusion time. 200 and 400 scans were measured at each diffusion time for fluid samples and core samples, respectively. Diffusion Editing is a technique for obtaining simultaneous diffusion and relaxation information in which the sample signal is "edited" by allowing diffusion to occur before relaxation data is collected (Hurliman, et al., 2002). The results can be displayed as a 2-D map or distribution of diffusion coefficients versus relaxation time, called a $D - T_2$ map. DE has been shown to aid evaluation of saturation, wettability, and fluid typing, as well as in the detection internal gradients. Internal gradients manifest as regions in the distribution with diffusion coefficients higher than the bulk diffusion coefficient of the fluids present. The magnitude of those internal gradients can be determined from the measured diffusion coefficient values. (Hurliman, et al., 2003).

RESULTS AND DISCUSSION

Fresh-State NMR T_2 distribution on the two fresh-state core plugs (gas space filled with base oil) at reservoir temperature and net confining stress were similar to what we had observed in the NMR logs, Figure 1, with a oil peak at about 150 ms. A comparison of T_2 distribution at ambient and reservoir temperatures of one of the fresh-state samples (#206) with pore fluid oil centrifuged from a nearby fresh-state core plug is shown in Figure 3. The oil T_2 peak in the rock is shifted to the left of the bulk oil T_2 peak indicating a non-water-wet rock. A comparison of the T_2 distribution at ambient temperature, 75°F, and reservoir temperature, 160°F, indicate no significant shift to longer relaxation

times for the oil in the rock compared to the shift of the bulk centrifuged oil sample from 264 ms to 602 ms, also supporting a non-water-wet rock. We calculate an internal gradient of about 230 G/cm using the multiple echo spacing T_2 measurement data on this fresh state core plugs.

This lack of temperature dependence is generally thought to indicate surface relaxation, oil is in direct contact with the portions of the core pore surface, as the dominant mechanism. (Kleinberg et al., 1994 & Foley et. al., 1996) (Different interpretation by Godefroy, et al., 2002) The relaxation mechanism in bulk oil is known to be temperature dependent whereas the relaxation mechanism at the rock surface has been shown to be only weakly temperature dependent. This does not necessarily indicate that the reservoir rock is oil wet or mixed wet, but that the wettability of the rock within the vicinity of the well bore may have been altered by the surfactants in the synthetic oil base drilling/coring mud.

T_2 spin-spin measurements respond to both rock wettability and internal gradients whereas T_1 spin-lattice measurements are not effected by the internal gradients and thus respond to only wettability alteration. Since T_1 measurements were not originally obtained on the two fresh state samples, T_1 and T_2 measurements were obtained on several new preserved samples (without adding base oil) and afterwards the samples were centrifuged to retrieve a sample of the contained oil for T_1 and T_2 measurements. There is a shift of about 100 ms to the left for the T_1 peak of the oil in the rock compared to the T_1 of bulk oil centrifuged from the rock. This indicates these fresh-state samples are not water-wet. Gas chromatograph analysis on these undiluted centrifuge oil samples obtained from preserved core plugs indicate they contain about 20% to 25% OBMF and thus 80% to 75% dead reservoir crude oil.

Extracted-State The two fresh-state core plugs were Dean-Stark extracted and continued extraction in a soxhlet with toluene, methanol, and tetrahydrofuran. The other four samples had been miscibly extracted with a series of solvents including toluene, methanol, and tetrahydrofuran. All six plugs then had T_2 measurements at ambient and reservoir temperature and often with multiple echo spacings at the following saturation states, 100% brine, S_{wi} by porous plate desaturation at 200 psi, S_{wi} +decane, and S_{wi} +base oil. The extracted samples have lower internal gradients, 50 to 100 Gauss/cm, than fresh-state samples or samples flushed with OBM filtrate; 150 to 230 Gauss/cm. The internal gradients are calculated from the multiple echo spacing data ($TE=0.3$ ms and 0.6 ms) of the peak mode for the 100% brine saturated samples or otherwise the HC peak mode. Mercury injection capillary pressure (MICP) measurements were obtained on the highest permeability sample, #54 (631 md) and the lowest permeability samples #206 (48 md). Combining the MICP data and the T_2 distributions at 100%

S_w , the surface relaxivity for water, ρ , was calculated to be 48 microns/sec for #54 and 56 microns/sec for #206.

As previously stated we saw no temperature dependence on the T_2 distribution for the fresh-state sample #206 (48md), Figure 3. We saw no temperature dependence on the T_2 distribution for the saturation state, S_{wi} + base oil. To obtain this saturation state, (Figure 4) the fresh-state sample was extracted, 100% brine saturated, desaturated on porous plate (S_{wi}), resaturated with decane, and then the decane replaced with the base oil used to make the OBM. The oil T_2 peak in the rock, S_{wi} + base oil, has shifted to the right compared to the fresh state, 400ms versus 250ms. The T_1 of the oil peak in the rock is still to the left of the T_1 of the bulk base-oil indicating that this sample is not water-wet even after extraction.

A similar comparison of temperature sensitivity and T_1 and T_2 for the higher permeability samples indicate slightly different behavior as illustrated in Figure 5 for sample #140 (345 md). The base oil peak in the rock is still to the left of the bulk base oil, but the peak does shift to the right at elevated temperature. The shift to the left of the base oil peak in the T_1 distribution of the rock compared to the bulk base oil is much smaller than was observed for the low permeability sample #206 (48 md). Assuming the magnitude of the T_1 shift of the base oil peak in the rock compared to bulk base oil is an indication of the degree of oil-wetness, then extracted sample #140 is less oil-wet than extracted sample #206. Consistent with this less oil-wetness, sample #140 also indicates a slight temperature dependent T_2 distribution (oil peak).

The results of Amott-Harvey (AH) wettability index test on two new miscibly extracted samples, #200 (684 md) and #477 (92 md), indicated that #200 with AH index of +0.83 was water-wet and #477 with an AH index of +0.12 was intermediate-wet. The NMR results on these plugs at S_{wi} +base oil saturation after the AH test are provided in Figure 6. The base oil T_2 ($TE=0.3ms$) peak is shifted more to the left for the intermediate oil wet sample than the water-wet sample. These results are generally consistent with NMR T_1 and T_2 measurements on core samples at fresh-state or S_{wi} +base oil, where samples with the low permeability show a separation between T_1 for bulk base oil and base oil saturated samples, while higher permeability samples indicate only slight to no separation between T_1 for bulk base oil and base oil saturated samples.

Impact of OBM filtrate preparation methods on NMR properties The preparation method to get the OBM filtrate has a big effect on its bulk relaxation time. As shown in Figure 7, T_2 relaxation time of the filtered supernatant (0.22 μ m filter paper) is much shorter than the corresponding base oil. For the filtrate obtained by pressing the whole mud through a 5 μ m filter paper, the T_2 relaxation time is much

closer to that of the corresponding base oil. However, for the first several drops of filtrate before the mud cake fully builds up, the T_2 relaxation time is closer to that of the filtered supernatant. The spurt loss that occurs while drilling should be analogous to the filtrate collected in the lab before the formation of a fully developed mud cake. Therefore we have investigated the properties of the OBMF (filtered supernatant) and its interaction with rock. We will refer to the OBMF obtained by filtering centrifuge supernatant at 0.22 micron as "filtered OBMF" ($T_1 > T_2$), while the filtrate obtained from pressing whole mud in a standard mud press with a 5 micron filter is referred to as "pressed OBMF" ($T_1 = T_2$).

We have measured the properties of filtered OBMF from six different mud samples taken over a period of several years. In all cases, the T_2 relaxation time is much shorter than the corresponding base oil, and the T_1 relaxation time of the filtered OBMF is about twice that of the T_2 relaxation time (Figure 7) while the corresponding base oil has $T_1/T_2 = 1$. All these three unusual behaviors were duplicated with the addition of small amount of finely dispersed magnetite 'ferrofluid' (Lisensky, 2003) in the OBM surfactant solution.

The viscosities of the pressed OBMF, filtered OBMF, and the base oil are similar. The DE plots indicate that filtered OBMF's have shorter T_2 relaxation times than the rest but all have similar diffusivities and thus the filtered OBMF deviates from the correlation between diffusivity and T_2 relaxation time for hydrocarbons (Lo, 1999, 2002; Freedman, et al., 2001), Figure 8.

Our hypothesis for these unusual behaviors for the filtered OBMF was the presence of paramagnetic particulates in the filtered OBMF that are absent from the pressed OBMF. Dynamic Light Scattering measurement (ZataPALS, Brookhaven Instruments) shows that the mean diameter of the particulate is 0.083 microns or 83 nm. To confirm that these particles contained paramagnetic ions, the filtered OBMF was contacted with 1 molar HCl solution for 24 hours and the HCl leach solution analyzed by Ion Coupled Plasma (ICP) (Optima 4300 DV, PerkinElmer Instruments). As shown in Figure 9, the T_2 relaxation time of the filtered OBMF increased after contacting with HCl, while the T_2 relaxation time of the HCl solution decreased. It suggests that some of the paramagnetic materials transfer from the filtered OBMF phase to the HCl leaching solution. The HCl solutions were analyzed before and after contacting the filtered OBMF. The ICP analysis indicates that the dominant paramagnetic elements in the sample are Fe (65 ppm) and Mn (8.6 ppm) with trace amounts of Co (1.1 ppm), Cu (0.7 ppm), and Ni (0.2 ppm).

The T_1/T_2 ratio and echo spacing dependence of T_2 of the filtered supernatant was compared with two model systems

(Figure 10). For a 3.2×10^{-4} mol/l solution of Fe^{3+} in 1M HCl, T_1/T_2 ratio is 1 and there is no echo spacing dependence of T_2 . The T_1/T_2 ratio is 2.0 for the core sample containing magnetite at S_{wi} +base oil and there is large echo spacing dependence of T_2 . The filtered supernatant has a T_1/T_2 ratio of 1.9 but no echo spacing dependence of T_2 .

The magnetic susceptibility of the filtered OBMF was diamagnetic, -0.8×10^{-6} cgs/g, indicating the bulk of the iron from ICP analysis must be paramagnetic and not ferromagnetic ($>10,000$ times larger magnetic susceptibility than paramagnetic iron). A sample of the OBM cake is paramagnetic, $+17.7 \times 10^{-6}$ cgs/g. The coarse material (+325 mesh) recovered from the whole mud with a strong magnet was found by visual inspection to consist of barite and metal flakes, while the fine fraction (-325 mesh) by XRD indicated barite and magnetite.

OBMF Flushed Cores So far we have focused on core plug saturation states 100%, S_{wi} +decane, and S_{wi} +base oil to help characterize the extracted rock that ideally has been returned to a more water-wet state. To investigate the interaction of OBM filtrate with the core at connate water saturation, we have flushed samples with filtered and pressed OBM filtrate.

Sample #206 (48 md) the previous focus of fresh-state (Figure 3) and S_{wi} +base oil (Figure 4) NMR studies was flushed at reservoir temperature with 2.5 pore volumes of filtered OBMF ($T_1 > T_2$) and then aged at room temperature for several months and finally flushed with base oil. T_1 and T_2 with multiple echo spacing measurements were obtained before the filtered OBMF flush and after the final base oil flush. (Figure 11). Also presented in Figure 11 is the DE plot that indicates high internal gradients. The apparent diffusion coefficient distribution is the projection of the DE map onto the diffusion coefficient axis. From the diffusion coefficient distribution, the local gradient strength distribution can be calculated as follows (Hürlimann, M. D., et al., 2003),

$$g_{\text{loc}} = \sqrt{D_{\text{app}}/D_0} \cdot g_{\text{ext}}$$

Where D_0 is the self diffusion coefficient, g_{ext} is the applied gradient strength in the DE measurements (13.2 G/cm). A diffusion coefficient cutoff of 1.0×10^{-3} cm²/sec is used for separating water and oil. The multiple ($TE=0.3$ ms and 0.6 ms) echo spacing data calculate an apparent gradient of 150 G/cm after the filtered OBMF flush, which was an increase from 74 G/cm prior to the filtered OBMF flush.

In an attempt to obtain a side-by-side comparison of the interaction of the both pressed and filtered OBMF with the core samples, two samples at a saturation state of S_{wi} plus base oil were flushed at reservoir temperature and stress with 3 pore volumes of OBMF and the T_2 distribution

monitored with time, Figure 12. Sample #165 (70 md) was flushed with pressed OBMF ($T_1 = T_2$) with a T_2 peak mode of 647ms (at 75 F) and the T_2 of the oil in the rock decreased from 567 ms immediately after flushing 3 pore volumes (time zero) to 276 ms after 108 hours. Sample #140 (345 md) after extraction and saturating with S_{wi} +base oil had a T_2 oil peak of 631 ms. The rock was then flushed with 3 PV of filtered OBMF ($T_1 > T_2=182$ ms at 75 F). The oil peak in the rock immediately decreased from 631 ms to 181 ms. Upon aging, the T_2 of the oil in the rock decreased from 181 ms immediately after flushing (time zero) to 86 ms after 64 hours.

Since the pressed OBMF does not contain detectable amounts of the paramagnetic particles, the shift from 567 ms to 276 ms for #165 is likely due to wettability alteration to more oil-wet character as a result of the surfactants in the OBM. The shift from 181 ms to 86 ms for #140 is likely due to a combination of increase in surface relaxativity and internal gradients from the paramagnetic particles depositing on the pore walls in addition to wettability alteration to more oil-wet character as a result of the surfactants in the OBM.

Wettability alteration of water-wet Berea

The effect of the OBMF on wettability alteration was further tested with strongly water-wet Berea core (Amott-Harvey: +1.0). 100% brine saturation of the Berea core # 83 and #71 were reduced to irreducible water saturation by centrifuge. Berea core #83 was then flushed with 7.7 pore volumes of the filtered OBMF and aged for 6 days at 194 °F. The Amott – Harvey wettability index measurement shows that it is altered to be intermediate – wet (Amott – Harvey index: 0.035). The internal gradient plot from DE measurements indicates an increase in gradient with flushing and aging, Figure 13.

Berea core # 71 was flushed with 10 pore volumes of base oil plus 2% NOVA surfactant and magnetite ferrofluid and aged for 6 days at 194 °F. The internal gradient plot from DE measurements indicates an increase in gradient with flushing and aging. Figure 14.

Log NMR data

The core-to-log calibration program demonstrates that the fresh-state core plugs appear to be oil-wet and have high internal gradients. We have also demonstrated with reservoir rock and Berea samples that the filtered OBMF alters the rock wettability to more oil-wet state and appears to increase internal gradients as the result of the invasion of both OBM surfactants and oil-wet submicron paramagnetic particulates. However, without a sample of un-invaded reservoir rock to analyze it is hard to assign how much of what we are observing is due to behavior of the reservoir rock aged with light crude oil containing 1% to 2% asphaltenes, or the result of OBMF invasion. We thought

that an NMR log in the water leg might help sort this out, since typically the rock below the oil-water contact is assumed to be water-wet.

One well in this Gulf of Mexico field had a wireline (CMR) NMR log over both the oil-leg and the water-leg, Figure 15. The wireline NMR tool was run approximately one week after drilling. As the well was drilled with oil base mud, it was expected that the wireline tool would indicate a classic bi-modal T_2 distribution, where the peak to the left indicates irreducible water volume and the peak to the right indicates the OBM filtrate bulk T_2 . It was observed that the peak associated with the bulk T_2 of the OBM filtrate was faster than expected as we had indicated early in this paper for the wireline (CMR) NMR log in the cored well (Figure 1). The CMR T_2 distributions in the sands were nearly identical in both the oil and water legs, with the oil peak at about 100 to 200ms. If the OBM filtrate entering the formation did not contain surfactants and submicron paramagnetic particulates and thus did not alter the response of the water-wet rock below the OWC, then the HC peak in the invaded zone seen by the CMR should have been out at about 1000ms. If the OBMF entering the formation above and below the OWC does contain surfactants and submicron paramagnetic particulates, the rock will be altered as a result of enhanced paramagnetic surface relaxativity, increased internal gradients. This wettability alteration to more oil wet conditions would result in similar oil peak position above and below the OWC.

This well that encountered an OWC happen to have the only LWD NMR log run in the field. This LWD-NMR tool was one of Schlumberger's earliest and was run as a field trial. There were problems with hole washout and tool rotation effecting the LWD NMR log over the sand intervals of interest. Tool motion may cause shifting to shorter relaxing times for long relaxing HC peaks (Morley, et al., 2002). About 2.5 days after drilling the well several LWD NMR wiper-pass logs obtained. As this is one of the earliest LWD NMR's run there have since been improvements in tool design and now motion detectors are incorporated as log quality control (LQC). Without such an LQC, a valid comparison between the drill pass and the CMR and/or wiper passes is not feasible. Only wiper trip LWD data was used for comparison to wireline data to exclude any uncertainty on data quality due to tool rotation effects.

A side-by-side comparison of the LWD wiper pass NMR log (2.5 days after drilling) and the CMR log (one week after drilling) is presented in Figure 16. There are 50-foot hydrocarbon bearing sand intervals above and below the shale interval at XX020ft. There was no wiper pass data below the OWC. The CMR log across these two sands intervals has apparently shorter relaxing HC peak T_2 of about 200ms, than observed with the LWD tool of about 500ms. One possible explanation would be that the flushed

zone was becoming more oil-wet due to the OBM surfactants and paramagnetic material.

Table 1 compares the acquisition parameters for the wireline and LWD runs. Only the long-wait time sequences are used in the presentation of the logs and subsequent data analysis. The LWD-NMR tool had three sequences; long wait-time, short wait-time, and bursts. The CMR tool had two sequences; long wait-time and bursts. The two key differences between the logs were the echo decay time, 180ms for the LWD_NMR and 600ms for the CMR, and the echo spacing, 800 microsecond the LWD_NMR and 200 microseconds for the CMR. The longer echo spacing of the LWD run is somewhat offset by a lower tool gradient assuming little contribution from the rock internal gradients.

Time domain analysis was used to compare the CPMG echo trains from both wireline and LWD tools and it clearly shows significantly faster decay for the wireline results (Figure 17). To improve the SN ratio, the 50 feet of hydrocarbon bearing sands above the shale zone at XX020ft were stacked. Both data sets have the same total echo decay time, 160ms, and only one out of every four echo amplitudes ($4 \times 200 = 800$ microseconds) were used from the CMR data so that both logs had the same number of echoes. Figure 17 shows that the echo decay data can be fit reasonably well with just a bi-exponential function. The echo decay data has been inverted with the biexponential fit and a 20 bin inversion. The resulting T_2 distributions are presented in Figure 18 and as indicated by the time domain data, the CMR has a faster hydrocarbon relaxation than the LWD-NMR. Accurate definition of the LWD HC peak is not possible due to the short echo decay time, 160 ms, causing the shape of the T_2 distribution to be undefined beyond about 400 ms.

The impact of the long echo spacing of the LWD_NMR tool and the potential reservoir internal gradients were assess by calculating the T_2 relaxation time for live crude oil at reservoir conditions using the tool parameters and the viscosity and GOR data from downhole sample PVT data. These data are presented in Figure 19. For these calculations, we have assumed that the tool and rock gradients are additive. (This may not be strictly valid.) These calculations indicate that for any rock internal gradient greater than about 5 G/cm, the LWD-NMR HC peak would be to the left of the CMR at the same rock gradient. Rock internal gradients would have to increase and wettability altered to a more oil-wet state between the time of the LWD and CMR measurements for LWD with TE of 800 microseconds to have longer relaxing HC peak than CMR with TE of 200 microseconds. The LWD-NMR does have a deeper depth of investigation, 2-3 inches, compared to the CMR with 0.5-1.5 inches as indicated in Table 1, and thus could be less altered. The AIT profile

analysis at time of CMR log indicate 20+ cm of invasion (Barber, 2004).

Discussion of Results The results of the NMR core measurements are summarized in Table 2. Remarkable features are the large internal gradients and T_1/T_2 ratio. The value of this ratio is typically 1.6 (Kleinberg, et al., 1993).

CONCLUSIONS

There appears to be at least five different mechanisms that could account for the apparent shift of the T_2 bulk live oil or OBM filtrate to much faster relaxing times observed in the LWD and wireline NMR logs:

1. Surfactants in the OBMF alter the rock wettability to more oil-wet.
2. Oil-wet submicron paramagnetic particles increase internal gradients and surface relaxativity.
3. Reservoir rocks naturally contain iron minerals including magnetite that could be expected to cause significant localized internal gradients.
4. The bulk OBMF containing submicron paramagnetic particles relaxes so much faster than the base oil or the pressed OBMF that the bulk OBMF relaxation dominates the rock-fluid response.
5. The oil T_2 relaxation time decreases with aging.

For this GOM field, mechanisms 1, 2, 4 and 5 are demonstrated by the core/fluid analysis and likely all five mechanisms are involved.

Conclusions from the core-to-log NMR calibration program are:

- Reservoir rock petrography, thin section point count, XRD, and SEM/EDX all indicate that these reservoir rocks naturally contain iron minerals including magnetite that one would expect to cause significant localized internal gradients. However there is no significant amount of dispersed clays.
- Fresh-state samples appear to be more oil-wet and have higher apparent internal gradients compared to extracted core plugs.
- Cores are typically not water-wet even after extensive extraction based on a comparison of the T_1 oil peak in core plugs at a S_{wi} +base oil saturation state and the bulk base oil T_1 peak.
- The NMR properties of the oil base mud filtrate depend on how mud sample is filtered:
 - a. A 0.22-micron filter cannot remove submicron paramagnetic particles, but a well-formed mud cake will.
 - b. Drilling spurt loss will likely contain submicron paramagnetic particles.
 - c. Since the T_2 and T_1 of the spurt loss is less than the

base oil it has the potential to affect the accuracy of NMR fluid typing.

- Flushing cores with OBMF containing submicron paramagnetic particles increase the oil-wetness of the rock and increase the surface relaxation and apparent internal gradients.

References

- Barber, T., 2004, personal communication on March 25.
- Chen, J.S., Hirasaki, G. J. and Flaum, M., 2004 "Study of Wettability Alteration from NMR: Effect of OBM on Wettability and NMR Response," 8th International Symposium on Reservoir Wettability, May 16-18, Houston, TX.
- Chuah, T. L., 1996, Estimation of relaxation time distribution for NMR CPMG measurements. Master thesis. Rice University, Houston, TX.
- Foley, I, Farooqui, S.A., Kleinberg, R.L., 1996, "Effect of Paramagnetic Ions on NMR Relaxation of fluids at solid Surfaces," *Journal of Magnetic Resonance A*, Vol. 123, pp. 95-104.
- Freedman, R., Lo, S.-W., Flaum, M. Hirasaki, G.J., Matteson, A., and Sezginer, A., 2001, "A New NMR Method of Fluid Characterization in Reservoir Rocks: Experimental Confirmation and Simulation Results," *SPEJ* (December) 452-464.
- Godefroy, S., Fleury, M., Defandre, F., and Korb, J.-P., 2002, "Temperature Effect on NMR Surface Relaxation in Rocks for Well Logging Applications," *J. Phys. Chem, B*, Vol. 106, pp. 11183-11190.
- Huang, C. C., 1997, "Estimation of Rock Properties by NMR Relaxation Methods". Master thesis. Rice University, Houston, TX.
- Hurlimann, M. D., and Venkataramanan, L., 2002 "Quantitative Measurement of Two-Dimensional Distribution Functions of Diffusion and Relaxation in Grossly Inhomogeneous Fields," *Journal of Magnetic Resonance*, Vol. 157, 31-42.
- Hurliman, M. D. *et al*, 2003, "Application of NMR Diffusion Editing as a Chlorite Indicator," paper SCA2003-26 presented at the International Symposium of the Society of Core Analysts held in Pau, France, 21-24 September.
- Kenyon, W., 1992 Nuclear magnetic resonance as a petrophysical measurement. *Nucl. Geophys.*, Vol. 6, 153-171.
- Kleinberg, R.L., Farooqui, S.A., and Horsfield, M.A., 1993, " T_1/T_2 Ratio and Frequency Dependence of NMR

Relaxation in Porous Sedimentary Rocks,” *JCIS*, Vol. 158, p 195-198.

Kleinberg, R. and Vinegar, H., 1996, “NMR Properties of Reservoir Fluids”, *The Log Analyst*, Vol. 37 (6), November – December.

Kleinberg, R. L., Kenyon, W. E. and Mitra, P.P., 1994, “Mechanism of NMR Relaxation of Fluids in Rock”, *Journal of Magnetic Resonance A*, Vol. 108, pp. 206-214.

Lisensky, G., 2003, “Synthesis of Aqueous Ferrofluid,” <http://www.mrsec.wisc.edu/edetc/cineplex/ffexp.html>, accessed on Nov.

Lo, S.W., 1999, Ph.D. thesis, Rice University, Houston, TX.

Lo, S.-W., Hirasaki, G.J., House, W.V., and Kobayashi, R., 2002, “Mixing Rules and Correlations of NMR Relaxation Time with Viscosity, Diffusivity, and Gas/Oil Ratio of Methane/Hydrocarbon Mixtures,” *SPEJ*, (March), 24-34.

Marschall, D.M. and Coates, G., 1997, “Laboratory MRI Investigation in the Effects of Inverted Oil Muds on Primary MRI Log Determinations,” SPE 38739, paper presented at the SPE ATCE, San Antonio, TX (5-8 October).

Morley, J. et al., 2002, “Field Testing of a New Nuclear Magnetic Resonance Logging-While-Drilling Tool,” paper SPE 77477 presented at the 2002 SPE Annual Technical Conference and Exhibition San Antonio, Texas, September 29 to October 2,

Rueslatten, H., Eidesmo, T., Lehne, K.A., and Relling, O.M., 1998, “The use of NMR spectroscopy to validate NMR logs from deeply buried reservoir sandstones,” *J. Pet. Eng. Sci.*, Vol.19, pp. 33-43.

Straley, C., Rossini, D., Vinegar, H., Tutunjian, P., and Morriss, C., 1994, “Core Analysis by Low Field NMR”, SCA paper 9404.

Zhang, G. Q., Huang, C.-C., and Hirasaki, G. J., 2000 "Interpretation of Wettability in Sandstones with NMR Analysis," *Petrophysics*, Vol. 41, No. 3, 223-233.

Zhang, G. Q., Hirasaki, G. J., and House, W. V., 2001 "Effect of Internal Field Gradients on NMR Measurements," *Petrophysics*, Vol. 42, No. 1 (Jan.-Feb.), 37-47.

Zhang, G.Q., Hirasaki, G.J. and House, W.V., 2003 “Internal Field Gradients in Porous Media,” *Petrophysics*, Vol. 44, No. 6 (Nov.-Dec.) 422-434.

ACKNOWLEDGEMENTS

The authors wish to thank and acknowledge their respective companies/organization for their support and approval to

publish this paper. The support of the Consortium on Processes in Porous Media is acknowledged. The contribution of Freddi Curby is acknowledged.

ABOUT THE AUTHORS

John L. Shafer has been a consultant to Reservoir Management Group for the past six years since retiring from Exxon after 19 nineteen years. Quantification of reservoir quality with low field NMR, core image analysis, and petrology has been the focus of his research for the past dozen years. He is a past President of the Society of Core Analysts (SCA), a chapter of SPWLA. John obtained a B.S. in Chemistry from Allegheny College in 1963, his Ph.D. in chemistry from University of California, Berkeley in 1970, and a M.S. degree in petroleum engineering from the University of Houston in 1992.

Jiansheng Chen currently is a Ph.D. candidate in the chemical engineering department at Rice University. His thesis work is on NMR surface relaxation, wettability and oil base mud drilling fluids under the direction of Dr. George J. Hirasaki.

Mark Flaum received a BEng in Chemical Engineering from McGill University, and is currently pursuing a doctorate at the Chemical Engineering Department of Rice University. His research focuses on the use of NMR diffusion-based measurements for characterization of porous media.

George J. Hirasaki received a B.S. Chemical Engineering from Lamar University and a Ph.D. Chemical Engineering from Rice University. George had a 26-year career with Shell Development and Shell Oil Companies before joining the Chemical Engineering faculty at Rice University in 1993. At Rice, his research interests are in NMR well logging, reservoir wettability, enhanced oil recovery, gas hydrate recovery, asphaltene deposition, emulsion coalescence, and surfactant/foam aquifer remediation.

Austin Boyd is the Program Manager of Petrophysics at Schlumberger-Doll Research in Ridgefield, Connecticut. Prior to moving to Ridgefield, he was Chief Petrophysicist for Schlumberger Middle-East & Asia, based in Dubai and Abu Dhabi and before moving to the Middle East was a Product Development Engineer in the NMR group at Schlumberger Product center in Sugar Land, Texas. He joined Schlumberger in 1981 as a Field Engineer after graduating with a BSc degree in Electrical Engineering from Dalhousie University.

Christian Straley Christian Straley has worked at Schlumberger-Doll Research as a research scientist for more than twenty years with interests in NMR. Much of the work that he did over that period was for interpretation development and support of CMR and MRX. Currently his

interests are refined oils, crude oils and live oils at elevated temperature and pressure. He received his BS from Washington and Lee University and his MS and PhD from the University of Delaware where he studied organic and physical chemistry.

Tim Borbas received a BS degree in petroleum engineering from West Virginia University in 1984. He joined Conoco Inc. (now ConocoPhillips) the same year. He has previously worked in the Exploration Production Technology section in Houston, Texas and Gulf of Mexico Region office in Lafayette, Louisiana. Tim currently is a staff engineer with ConocoPhillips in the US Lower 48 organization. His duties include open and cased hole

petrophysical support for Gulf of Mexico deep water projects.

Chuck Devier

Chuck Devier is Director of Operations for PTS Laboratories, Inc. being responsible for all aspects of laboratory operations, including working with clients to develop specific laboratory procedures and protocols, along with technical and quality control evaluation. His 29 years in routine and special core analysis include laboratory management, Research and Development, and core-log integration. His experience includes both US and International areas. Chuck graduated with a BS Degree in Geology from Washington State University in 1974.

Table 1: Comparison of LWD and wireline NMR parameters

Parameter	LWD NMR (wiper pass)	Wireline NMR
Wait Time (seconds)	4.8	15.6
Echo Spacing (μsec)	800	200
Number of Echoes	200	3000
Field Gradient (G/cm)	3	20
Estimated DOI (inches)	2-3	0.5-1.5
Logging Speed (fph)	60	800
Time after drilling	2.5 days	1 week

Table 2: Summary of core NMR data

Sample#	Perm md	State	Fluid	A-H	Temp F	T1 ms	T2(0.3) ms	T1/T2	G G/cm
206	48	fresh	OBM+crude		160		250		230
206	48	extracted	base oil		160	1000	400	2.5	74
206	48	flushed w filtered OBM	filtered OBM		160		231		89
206	48	flushed + aged at room temp. for months	base oil		75	491	165	3.0	152
140	345	extracted	base oil		75	948	501	1.9	78
140	345	extracted	base oil		160		631		
140	345	flushed w filtered OBM (182 ms at 75 F)	filtered OBM		160		181		
140	345	flushed + aged at 160 F for 64 hours	filtered OBM		160		86		
165	70	extracted	base oil		160		568		
165	70	flushed w pressed OBM (647 ms at 75 F)	pressed OBM		160		567		
165	70	flushed + aged at 160 F for 108 hours	pressed OBM		160		276		
477	92	extracted	base oil	0.12	82	831	301	2.8	139
200	684	extracted	base oil	0.83	82	937	414	2.3	116
Berea		Swi with base oil	base oil		82		564		18 (LM)
Berea 83	96	7.7 PV flush w filtered OBM (220 ms), 6 days	filtered OBM	0.04	82		180		25 (LM)
Berea 71	84	10 PV, 2% NOVA + magnetite (70 ms), 6 days	2% NOVA, magnetite	-0.52	82		58		27 (LM)

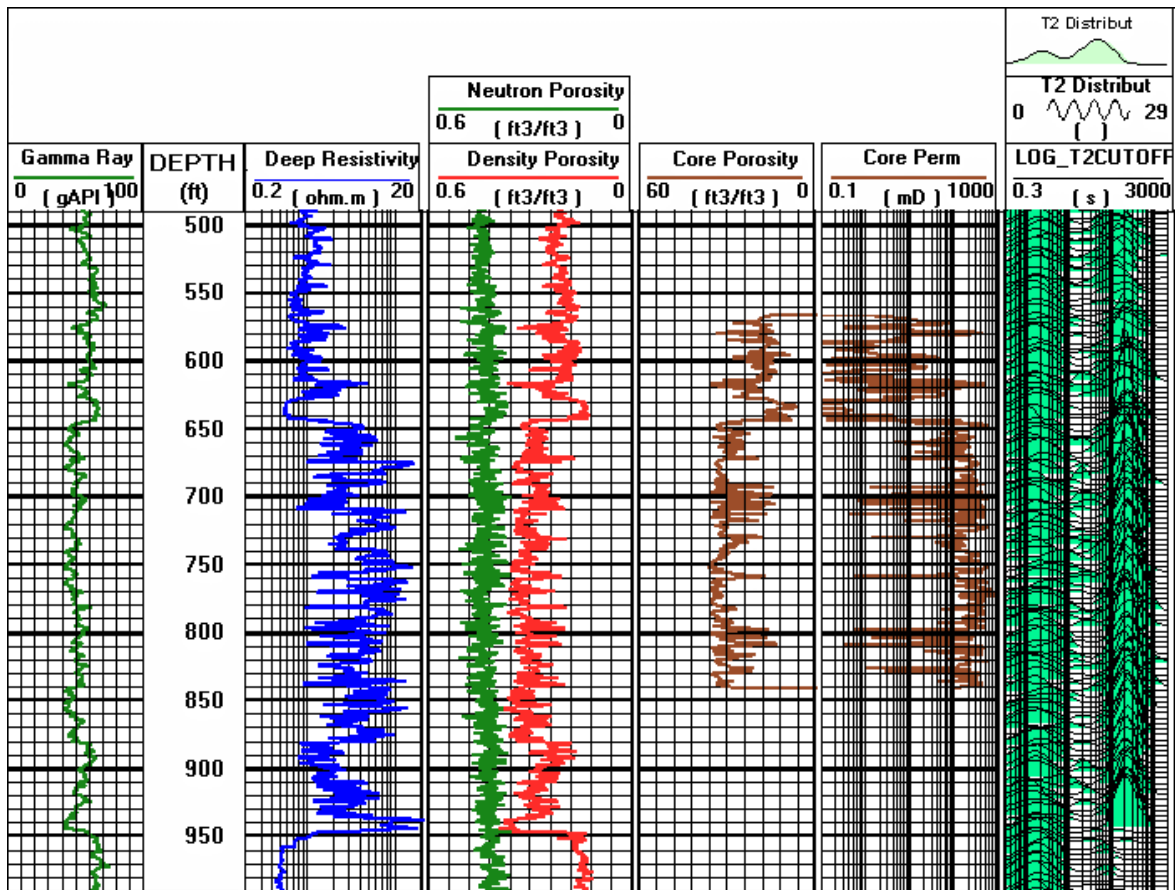


Figure 1 Log of cored well

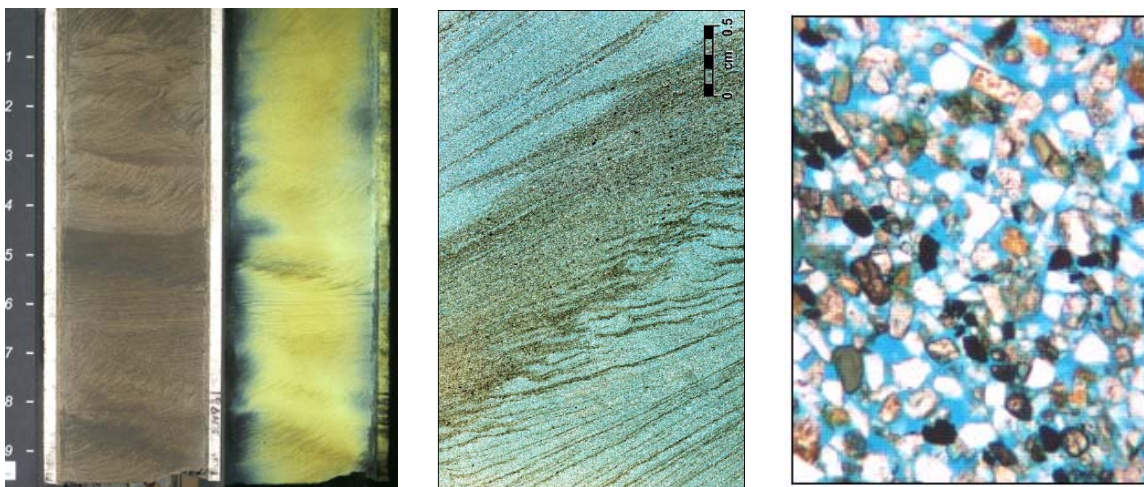


Figure 2 Reservoir heterogeneity on core and plug scale. Dark grains are heavy minerals, possibly containing iron.

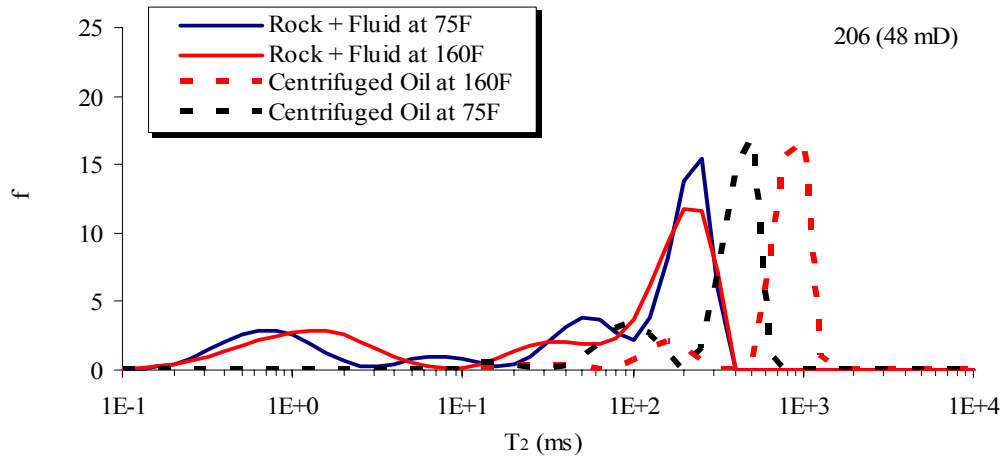


Figure 3 T_2 distributions of “fresh state” core plug 206, temperature dependence

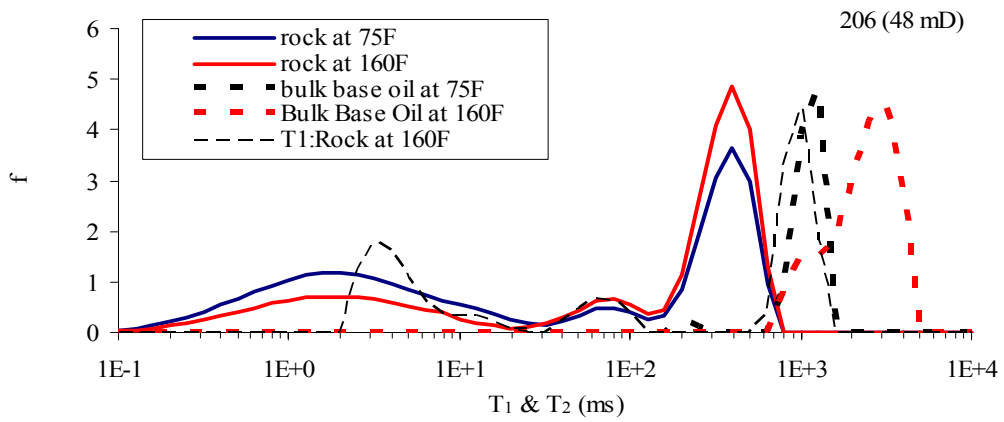


Figure 4 T_2 distributions of “extracted state” core plug 206, temperature dependence

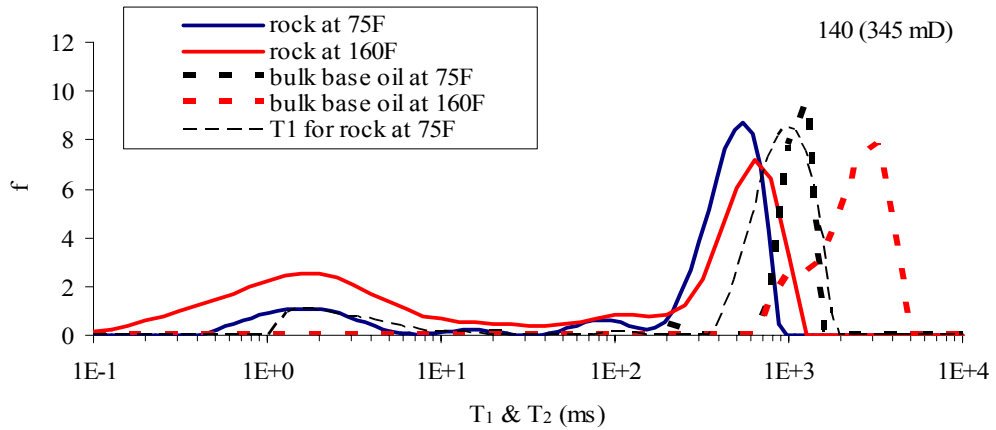


Figure 5 T_2 distributions of “extracted state” core plug 140, temperature dependence

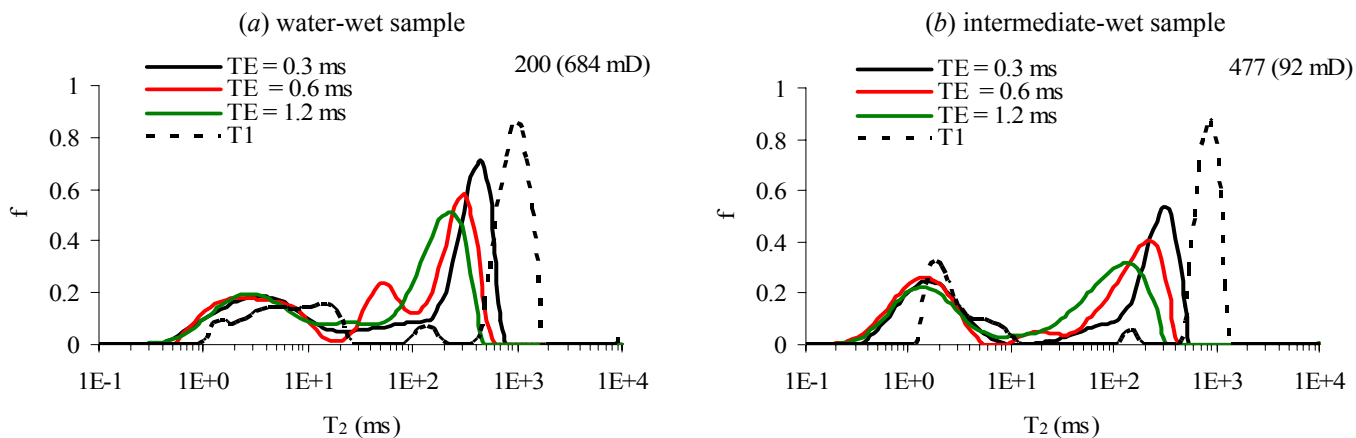


Figure 6 T_1 and T_2 (at multiple echo spacing) of water-wet sample ((a), AH=0.83) and intermediate-wet ((b), AH = 0.12) sample

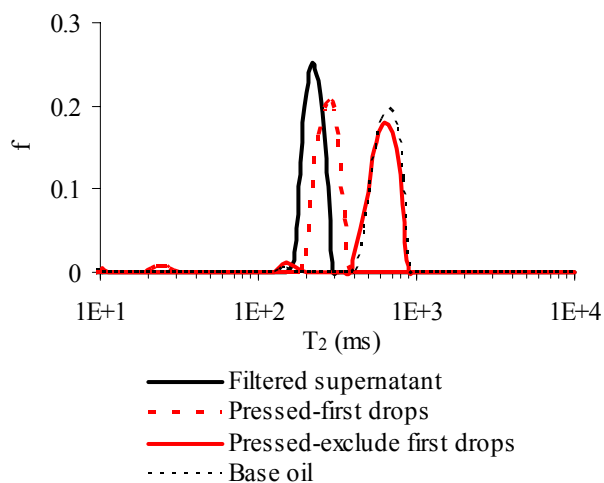


Figure 7 Impact of OBMF preparation methods on NMR relaxation time.

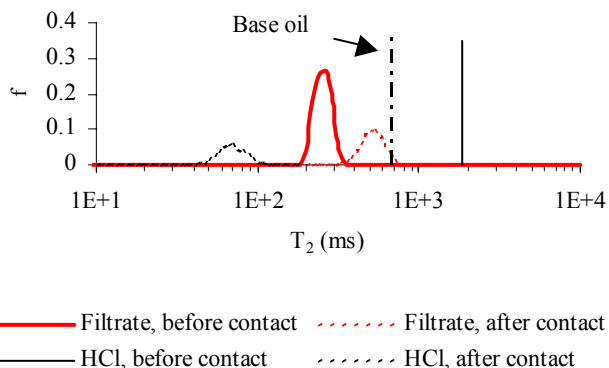


Fig. 9 HCl leaching of paramagnetic particulate from the filtrate

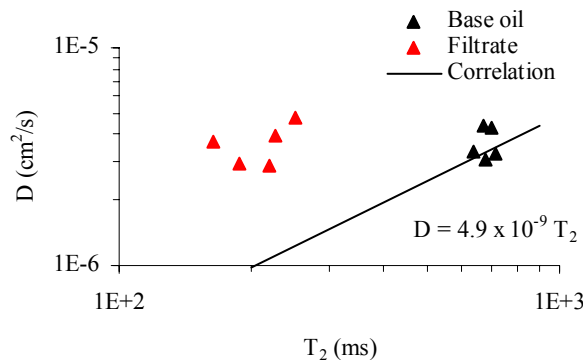


Figure 8 Deviation from the correlation between D and T_2 for the filtrates

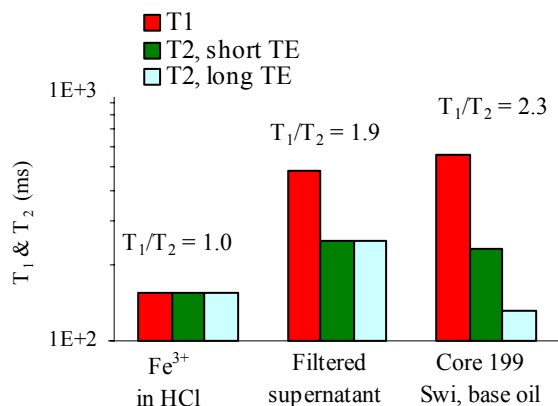


Fig. 10 T_1/T_2 ratio and echo spacing dependence of T_2

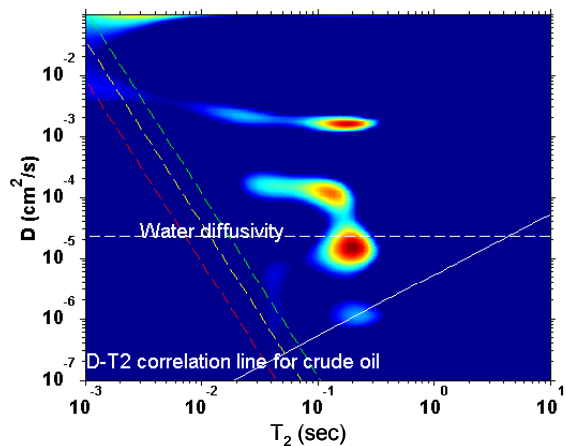


Figure 11 (a) Diffusion editing of core 206 at S_{wi} with base oil post OBMF flushing

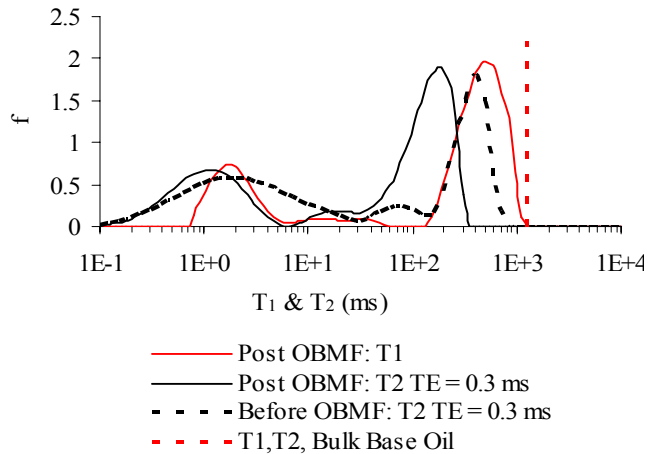


Figure 11 (b) T_1 and T_2 relaxation time distribution of core 206 at S_{wi} with base oil before and post OBMF flushing

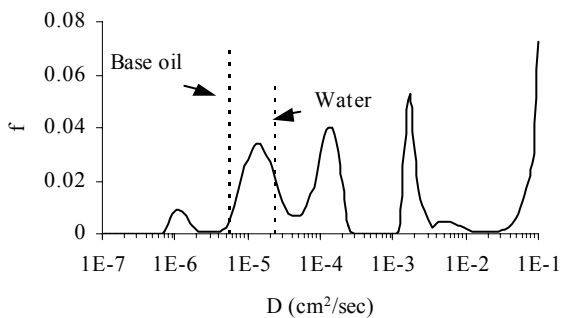


Figure 11 (c) Diffusivity distribution, projection to the diffusivity axis from Figure 11 (a)

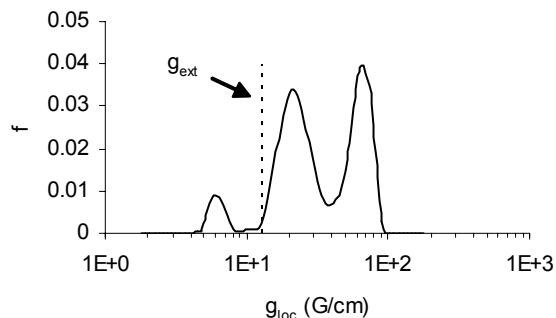


Figure 11 (d) Local gradient distribution experienced by oil

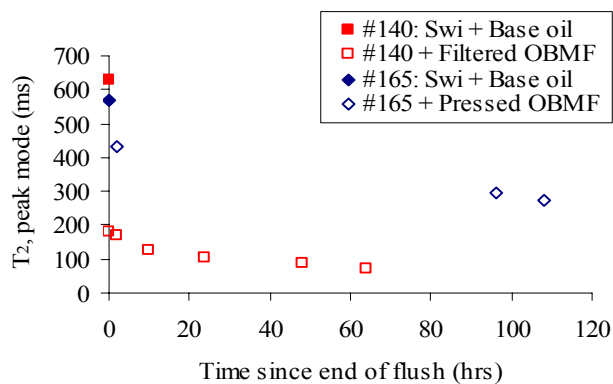


Figure 12 Monitor of T_2 with time after flushing with filtered and pressed OBMF

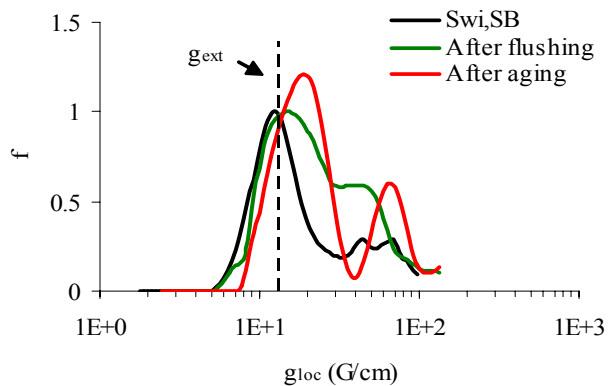


Fig. 13 Internal gradient strength of Berea core after flushing with filtered OBMF and after aging (#83)

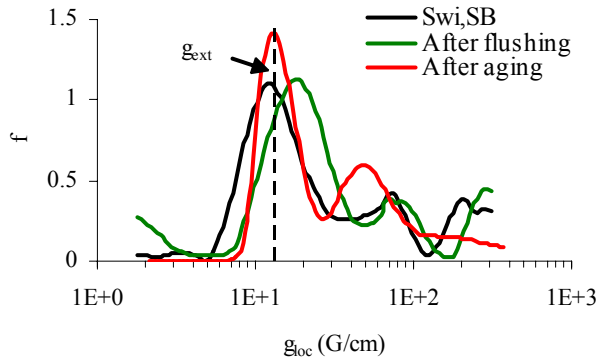


Fig. 14 Internal gradient strength of Berea core after flushing with oil containing surfactant and magnetite and after aging (# 71)

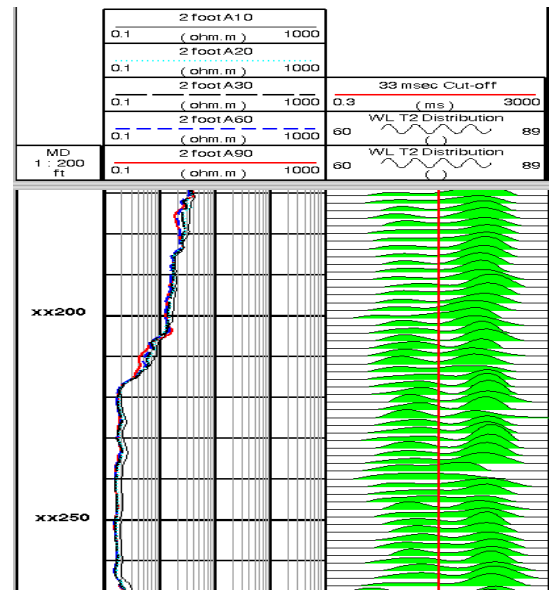


Figure 15 Wire line (CMR) Log over both the oil-leg and water-leg

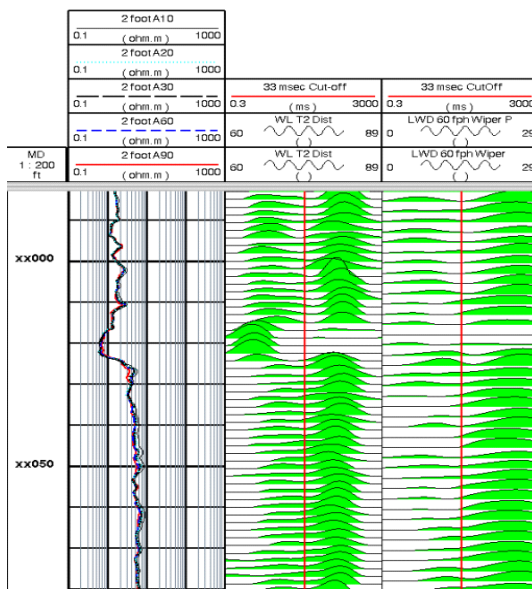


Figure 16 Comparison of CMR (left) and LWD (right)

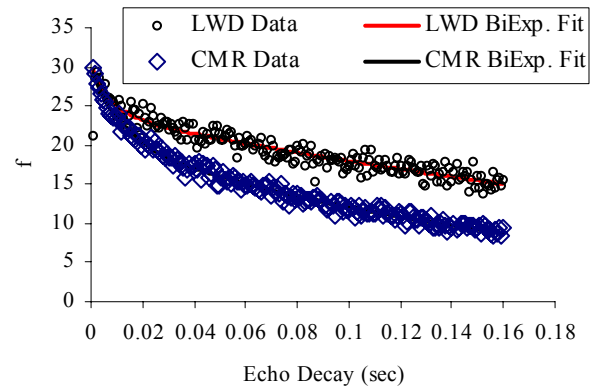


Figure 17 Stacked echo data for LWD wiper pass and CMR

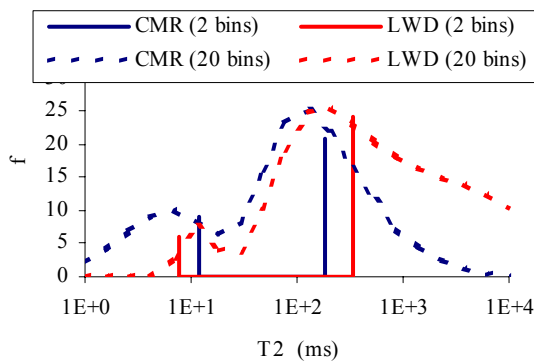


Figure 18 Comparison of LWD NMR and CMR

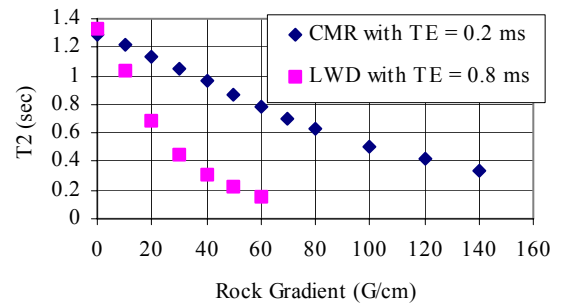


Figure 19 T_2 for bulk live crude oil